Proceedings of the Research Institute of Atmospherics,
Nagoya University, vol.30(1983)

RESEARCH REPORT

A METHOD OF ANALYSIS IN THE SOLAR OCCULTATION MEASUREMENTS

Masumi TAKAGI and Yutaka KONDO

Abstract

On the basis of the solar occultation method we measured in recent years the densities of aerosol and ozone in the lower stratosphere by balloon-borne sun-photometers. In reducing the observed optical depth to the extinction profile we have improved analytical procedures. It is essential in the procedures to estimate as accurately as possible the effect of refraction and absorption of sunlight in the atmosphere. This report describes a practical technique which is commonly applicable to the analysis of solar occultation measurements.

1. Introduction

In recent years we have observed the density profiles of aerosol and ozone in the upper troposphere and the lower stratosphere by using balloon-borne equipments (Kondo and Takagi, 1980; Kondo et al., 1978, 1982a, 1982b). The method of observations is based on the solar occultation by the earth's atmosphere. A similar method to this is utilized in the remote sensing plan of the global distribution of stratospheric aerosol and ozone by EXOS-C satellite which will be launched in February 1984. In connection with these observations we have developed an analytical procedure which derives as accurately as possible the extinction profile of aerosol or ozone from the observed

optical depth.

In the analysis of this method it is important to estimate the effect of refraction and absorption of sunlight when it passes through the atmosphere. Miller (1967) reported a reasonable model to compute the atmospheric attenuation in reducing rocket or satellite data. Wang et al. (1981) dealt with formulation of optical path for the case when the atmospheric refraction is significant. In taking the finite size of solar disk into consideration these expressions are not always consistent and appropriate for computation. Described in the present report is a technique which involves determination of optical path under the influence of atmospheric refraction, the total mass contributing to extinction along the determined optical path, correction of the differential refraction, and the effect of finite solar disk size. This technique is more practical and convenient for data reduction than those reported until now, and is commonly applicable to the analysis of solar occultation measurements.

2. Determination of optical path

General idea on the solar occultation measurements of atmospheric constituents is shown in Fig. 1 by the geometrical arrangement of the sun, the earth's limb, and the photometer on board balloon, rocket or satellite. The sunlight received with the photometer is attenuated when it passes through the earth's limb atmosphere. The atmospheric components which mainly concern the solar ray attenuation depend on wavelength. At the wavelength not included in absorption bands of minor gas constituents such as ozone and nitrogen dioxide, the attenuation of light results from Mie scattering of aerosols, Rayleigh

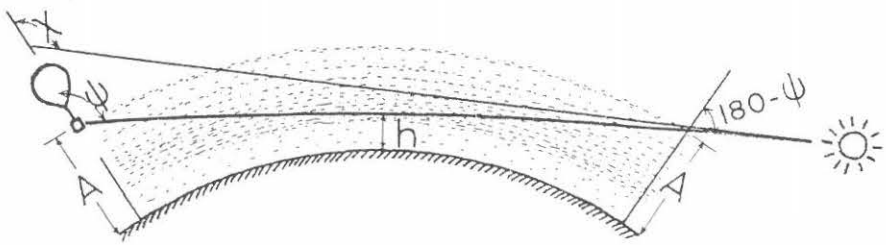

Fig. 1. Geometrical arrangement in solar occultation measurement of the atmosphere.

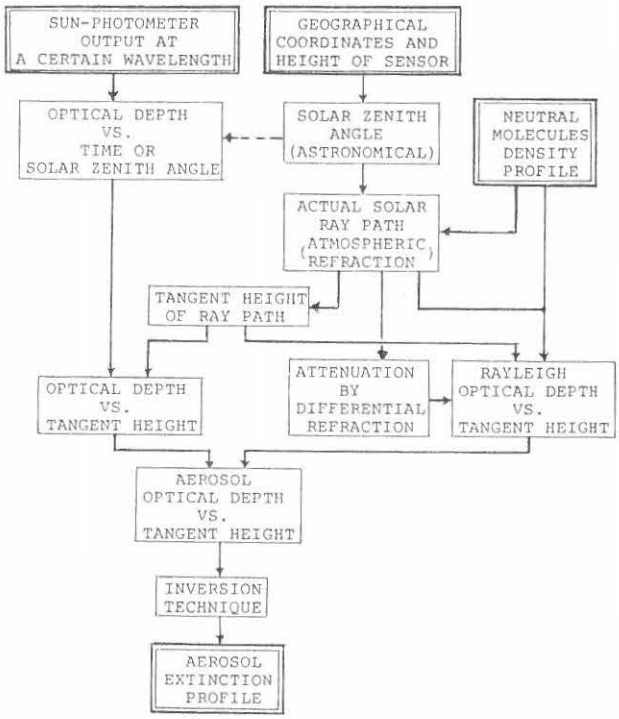

Fig. 2. Procedure of reduction of solar occultation data to aerosol extinction profile.

scattering of neutral air molecules, and the differential atmospheric refraction in the vicinity of the earth surface. The procedure for obtaining the aerosol extinction profile in this occasion is shown in Fig. 2 as an example.

The data necessary at first are of course the measured values of sunlight intensity. The intensity i is compared with the reference i_o, which is usually the solar intensity at a time when the solar zenith angle is so small that the atmospheric attenuation is negligible, and the ratio of them determines the optical depth as $\tau = \ln(i_o/i)$. The location and time of observation are necessary to derive the solar zenith angle. The density profile of neutral air molecules, which is indispensable for the computation of atmospheric absorption and refraction, is favorable to be measured at the same time as the observation, but the standard atmosphere is usuable in most cases when some errors are allowed in comparison with uncertainties arising from the optical depth measurements and during the analytical procedures.

The optical depth τ is thus given as a function of measured wavelength λ and solar zenith angle χ. The first step to convert the optical depth $\tau(\lambda, \chi)$ into the extinction profile $\beta(\lambda, z)$ is to deter-

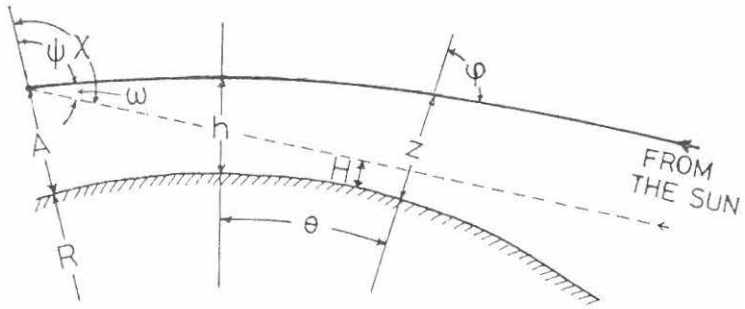

Fig. 3. Geometry of the sensor, the earth's limb and the solar ray path.

mine the solar ray path actually refracted by the altitude variation of atmospheric density. The parameters used in the computation and indicated in Fig. 3 are as follows.

R: radius of the earth

A: altitude of the sensor

h: tangent height of the actual ray path

H: tangent height of the ray path without consideration of refraction

z: altitude of a certain point on the actual ray path

χ: astronomical solar zenith angle

ψ: apparent solar zenith angle actually seen from the sensor

ω: refraction angle, $\omega = \chi - \psi$

ϕ: angle between the ray path and vertical line at a certain point on the ray path

θ: angular distance indicating the position of a certain point on the ray path. It is convenient for the general treatment to take the origin of θ at the tangential point on the ray path.

Considering a minute angle step $\Delta\theta$ as shown in Fig. 4, the ray path altitude z_i, corresponding to the position θ_i defined as $\theta_i = i \cdot \Delta\theta$ ($i = 0, 1, 2, \cdots\cdots$), is determined in order by the following equations. Based on the sine theorem,

$$z_{i+1} = (z_i + R) \frac{\sin \phi_i}{\sin (\phi_i - \Delta\theta)} - R \tag{1}$$

$$\Delta l_i = (z_i + R) \frac{\sin \Delta\theta}{\sin (\phi_i - \Delta\theta)} \tag{2}$$

and from the Snell's law which assures the conservation of the value of $(z_i + R)\, n_i \sin \phi_i$,

$$\phi_{i+1} = \sin^{-1} [\frac{n_i}{n_{i+1}} \sin (\phi_i - \Delta\theta)] \tag{3}$$

where Δl_i is the minute ray path length corresponding to $\Delta\theta$, and n_i

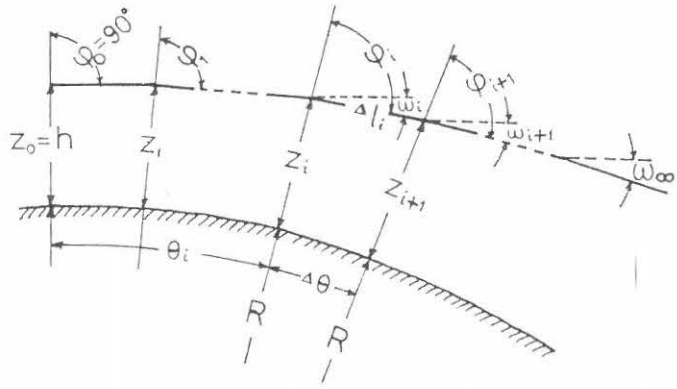

Fig. 4. Indication for steps of the solar ray path tracing.

and n_{i+1} are the refractive indices at the altitudes of z_i and z_{i+1}, respectively. The refractive index is a function of wavelength in a strict treatment (refer to Appendix), but the wavelength errors are not sensitive in ray tracing (Snider and Goldman, 1975). As far as we treate the wavelengths in visible or near infrared region, it is enough for ray tracing to use the value at $\lambda = 600$ nm. Thus the refractive index for the atmospheric density $\rho(z_i)$ is

$$n_i = 1 + 2.77 \times 10^{-4} \cdot \rho(z_i)/\rho(z=0). \tag{4}$$

The four equations above are fundamental for tracing the ray path. We can determine the ray path step by step after starting from $z_o = h$ and $\phi_o = 90°$. The refraction angle at the height z_i on the ray path is given by

$$\omega_i = \phi_i + \theta_i - 90°. \tag{5}$$

Let us then consider the total mass which contributes to the absorption of light. If the density of the k-th constituent of the atmosphere (for examples, neutral air molecules, ozone, nitrogen dioxide, or may be aerosol in some cases) at the height z_i is denoted as $\rho_i{}^k$, the line integral of mass density of the k-th constituent from h to z_i along the ray path is

$$M_i{}^k = \sum_{i=o}^{i-1} \rho_i{}^k \cdot \Delta l_i \tag{6}$$

For air molecules we denote hereafter as M_i and ρ_i without the suffix k.

In the balloon observations the sensor altitude is in most cases still inside the region subject to atmospheric absorption and refraction. Representing the values at the sensor altitude by adding the suffix A, for the values of ϕ_A, ω_A, and M_A we may interpolate from the

values of ϕ_i, ϕ_{i+1} and others when z_i and z_{i+1} contain the sensor altitude A between them. The apparent solar zenith angle actually seen from the sensor is given by

$$\psi = 180° - \phi_A. \tag{7}$$

In the side toward the sun the computation is continued until z_i exceeds a previously set height z_{max} (a height above which the absorption and refraction are negligible within the required accuracy, and the height of 50 km usually satisfies the above demand). The values here are ϕ_∞, ω_∞, and M_∞. Hence the total refraction angle along the overall path length from the sun to the sensor is $\omega = \omega_A + \omega_\infty$, and the total mass density line integral is $M = M_A + M_\infty$, and the astronomical solar zenith angle is given by $\chi = \psi + \omega$.

In the case of rocket or satellite observations, the sensor is outside the absorption region of the atmosphere. Then simply $\omega = 2\omega_\infty$ and $M = 2M_\infty$.

The procedure thus makes up the sets of $\chi(h)$, $\psi(h)$, and $M(h)$ as functions of the tangent height h.

An alternative procedure where the computation starts from the sensor position with a parameter ψ to make up the sets of $h(\psi)$, $\chi(\psi)$, and $M(\psi)$, and another procedure starting from z_{max} with a parameter $\phi(z_{max})$ properly chosen to make up the sets of $h(\phi)$, $\psi(\phi)$, $\chi(\phi)$, and $M(\phi)$ are also possible. But the procedure first described is more simple and better in general use than the others.

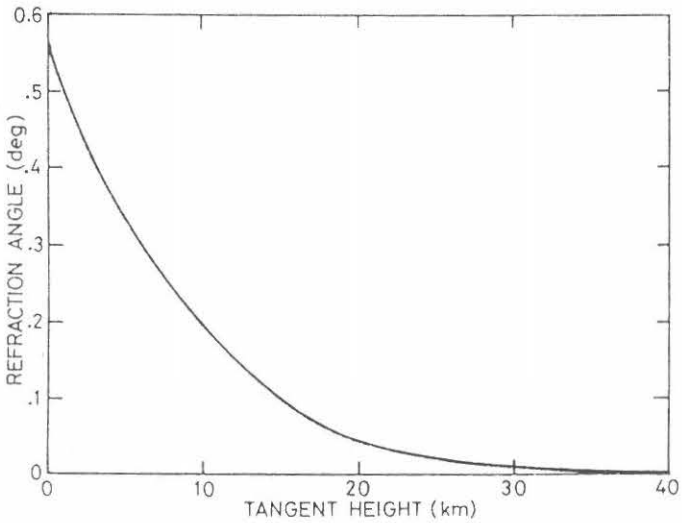

Fig. 5. Refraction angle seen from the tangent height indicated in the abscissa.

Fig. 5 shows the result of ω_∞ computed by using the standard atmosphere. The refraction angle of ray path which starts horizontally from the earth surface is about 0.56°(= 34') and nearly equal to the diameter of solar disk of 32'. For the ray path starting from the tangent height of 10 km the refraction angle is 0.20°. For the 20 km tangent height it is still 0.05° and the value significant enough to be considered in the analysis.

Figs. 6 and 7 are examples which compare the tangent height in

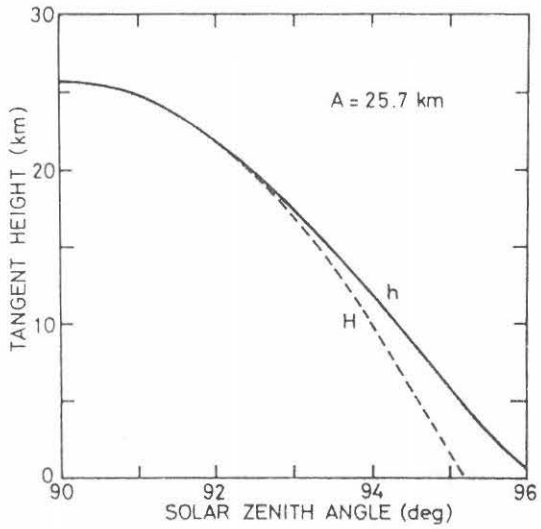

Fig. 6. Comparison of tangent height in actually refracted ray path (h) and that neglecting refraction (H) seen from balloon observation altitude.

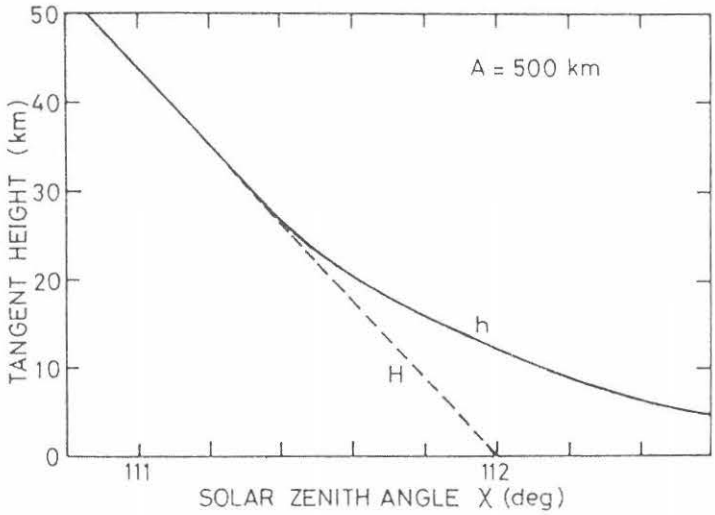

Fig. 7. Comparison of tangent height in actually refracted ray path (h) and that neglecting refraction (H) seen from satellite observation altitude.

actually refracted ray path (h) and that neglecting the refraction(H). In Fig. 6 the balloon observation height of 25.7 km as an example makes the difference of about 2 km between h and H at the height of 10 km. The difference is much larger in the case of satellite observation in Fig. 7, where A = 500 km, than balloon observations. It is obvious that this tangent height difference has a decisive importance in obtaining the required vertical resolution of the order of 1 km.

3. Attenuation caused by differential refraction

When the parallel flux from the sun passes over the vicinity of the earth surface, the lower side of flux passing through denser atmosphere is more refracted than the upper side of flux passing through thinner atmosphere. This means that the parallel flux diverges because of the height dependence of refractive index and that the flux density goes to diminish after passing over the earth's limb. Seeing the sun inversely from the sensor side the divergence of flux causes shortening in vertical in the appearance of solar disk. This is a well known phenomenon on the photographs of the sun and the moon taken from spacecrafts when the sun or the moon is seen just above the earth's horizon.

Now let the solid angle corresponding to a minute area ΔS on the solar disk be $\Delta\Omega$ in the case of no refraction. If $\Delta\Omega$ is changed to $\Delta\Omega'$ by the differential refraction described above, the light flux density from ΔS suffers attenuation (Born and Wolf, 1970) by the factor

$$D = \frac{\Delta\Omega'}{\Delta\Omega}. \tag{8}$$

Hence if the field of view of the sensor includes the whole solar disk, the light intensity received with the sensor is attenuated by the integral mean of D-factors all over the solar disk.

If the field of view is so narrow to be restricted in a small part on the solar disk, the condition above has a different situation. Because the field of view on the solar disk effectively expands according to the divergence of flux (according to the disk flattening), the light intensity received does not change if the radiation from every part of the disk is uniformly distributed. Actually the brightness distribution on the disk shows limb darkening and occasional big spots, and it is considerably troublesome to treate the light from edge or spot portion of the disk. In satellite observations it is

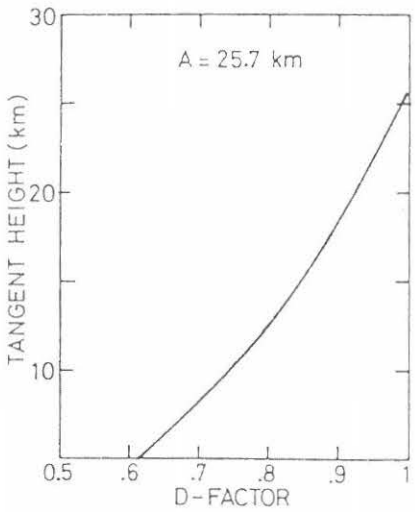

Fig. 8. Attenuation factor D versus tangent height for balloon observation, A = 25.7 km.

necessary to use much smaller light source than the whole solar disk in order to get sufficient height resolution. In the design of EXOS-C satellite the field of view divides the solar disk into about 30 x 30 sections, and therefore the D-factor correction usually may not be considered.

In balloon observations the field of view is usually so designed as to include the whole disk from the simplicity of equipment because the low altitude of sensor assures a good height resolution even for viewing the whole disk of 32' in diameter. The correction of D-factor in this case is as follows. The solar disk is divided into narrow sections parallel to the earth's horizon. Corresponding to the j-th section the apparent solar zenith angle width $\Delta\psi_j$ and the astronomical solar zenith angle width $\Delta\chi_j$ are computed by the procedure described in the former paragraph. The coefficient of attenuation for the j-th section is clearly

$$D = \frac{\Delta\psi_j}{\Delta\chi_j} . \tag{9}$$

Fig. 8 shows an example of D-factor computation for A = 25.7 km. For the ray path passing at 10 km tangent height the D-factor reaches to about 0.74.

4. Optical depth

The optical depth is an expression involving all the effects which attenuate the light intensity. In the former paragraphs, we obtain the actual ray path and at the same time the value of mass line integral of the k-th constituent M^k and the attenuation factor D corresponding to h, ψ or χ. These values are of course different according to different positions on the solar disk. Hence the light intensity from each of the solar disk divided into m pieces is summed up over the whole disk, before and after passing through the atmosphere, respectively. Then the two sums are compared.

The brightness distribution on the solar disk has been given in reference with coordinates (x, y) and wavelength λ (Allen, 1976). We denote it here as $I(\lambda, x, y)$. The brightness of the j-th section is

$$G_j(\lambda) = \iint_{S_j} I(\lambda, x, y)\, dx\, dy \tag{10}$$

where S_j means the region of the j-th section. The overall disk brightness is

$$G(\lambda) = \sum_{j=1}^{m} G_j(\lambda) \ . \tag{11}$$

The intensity received with the sensor from the j-th section is

$$H_j(\lambda) = G_j(\lambda) \cdot D(\chi_j) \cdot \exp\left[- \sum_k \sigma_k(\lambda) \cdot M_j^{\,k} \right] \tag{12}$$

where $\sigma_k(\lambda)$ is the extinction cross section of the k-th constituent at a wavelength λ. The total received intensity is

$$H(\lambda) = \sum_{j=1}^{m} H_j(\lambda) \ . \tag{13}$$

Because the total optical depth $\tau^*(\lambda)$, which will be obtained in the observations, is defined by

$$\frac{H(\lambda)}{G(\lambda)} = \exp\{-\tau^*(\lambda)\} \tag{14}$$

then

$$\tau^*(\lambda) = -\ln\left[\frac{\sum_j G_j(\lambda) \cdot D(\chi_j) \cdot \exp\{ - \sum_k \sigma_k(\lambda) \cdot M_j^{\,k} \}}{\sum_j G_j(\lambda)} \right] . \tag{15}$$

For the Rayleigh optical depth including the effect of differential refraction,

$$\tau_R(\lambda) = -\ln\left[\frac{\sum_j G_j(\lambda) \cdot D(\chi_j) \cdot \exp\{-\sigma_R(\lambda) \cdot M_j\}}{\sum_j G_j(\lambda)} \right] \tag{16}$$

where $\sigma_R(\lambda)$ is the Rayleigh scattering cross section. As the actual observations are carried out by using interference filter with a certain wavelength bandwidth $\lambda_1 \sim \lambda_2$, the cross section is given as the

integral mean between λ_1 and λ_2. Then actually used in the computation in Eq. (16) is

$$\langle\sigma_R\rangle = \int_{\lambda_1}^{\lambda_2} \sigma_R(\lambda)\cdot T(\lambda)\Phi(\lambda)\varepsilon(\lambda)\, d\lambda \,/\, \int_{\lambda_1}^{\lambda_2} T(\lambda)\Phi(\lambda)\varepsilon(\lambda)\, d\lambda \qquad (17)$$

where $T(\lambda)$ is transparency of filter, $\Phi(\lambda)$ is solar flux, and $\varepsilon(\lambda)$ is the sensitivity of photometer.

5. Vertical profile of extinction coefficient

In the near infrared region longer than 800 nm, the optical depth almost completely depends on Mie scattering of aerosols and Rayleigh scattering, including the effect of differential refraction, of neutral air molecules. The observed optical depth τ_{ob} consists of the above two. Using $\tau_R(\lambda)$ defined in Eq. (16) the aerosol optical depth τ_a is

$$\tau_a(\lambda) = \tau_{ob}(\lambda) - \tau_R(\lambda) \ . \qquad (18)$$

On the other hand the optical depth is expressed as follows.

$$\tau(h) = 2\int_h^A \beta(z)\cdot\frac{dl}{dz}\cdot dz + \int_A^{z_{max}} \beta(z)\cdot\frac{dl}{dz}\cdot dz \qquad (19)$$

where $\beta(z)$ is the extinction coefficient and l is the length along the ray path. The second term of the right side may actually be substituted by the measured optical depth when the apparent solar zenith angle is $180° - \psi(h)$ as shown in Fig. 1. Thus the values of $\tau_a(h, \lambda)$ expressed as a function of tangent height h can be inverted by, for example, the onion peeling method (Fynat and Smith, 1980; Pepin, 1977) to obtain the vertical profile of extinction coefficient $\beta_a(z, \lambda)$ of aerosols.

The procedure in this way is consistently based on the ray tracing in the atmosphere above the curved earth surface.

Lastly we add the method of obtaining the profile of minor gas constituents, for ozone as an instance. There is an absorption band of ozone centered at 600 nm. The optical depth observed within this absorption band is the sum of τ_{O_3}, τ_a, and τ_R. To deduce τ_{O_3} from τ_{ob}, therefore, information of τ_a and τ_R at this wavelength λ_0 are needed. A method of estimating τ_a at λ_0 is to extrapolate, considering the wavelength dependence of τ_a, from τ_a at the wavelength outside the absorption band, for example at 1000 nm, obtained in such a manner as

mentioned above. The results of ozone density measurements by using this method is described in the other report (Kondo et al., 1983).

6. Concluding remarks

It is emphasized in the solar occultation measurements of the atmospheric minor constituents that the effect of atmospheric refraction is important to obtain accurate vertical distribution. Consideration for the refraction is essential in the case when we deal with constituents in the altitudes lower than 30 km. To attain a good height resolution it is also important that the solar disk cannot be treated as a point light source. The procedure described in this report is consistently based on the ray path tracing under the influence of atmospheric refraction, and is intended for making the errors arising in the course of data reduction as small as possible.

Appendix

The Rayleigh scattering cross section needed for the computation is given by the following equations.

$$\sigma_R(\lambda) = \frac{32\pi^3 (n-1)^2}{3N^2\lambda^4} \cdot \delta$$

$$\delta = (6 + 3\Delta)/(6 - 7\Delta) \qquad (\delta: \text{depolarizing factor})$$

$$N = 2.547 \times 10^{19} \ \text{cm}^{-3}$$

$$n - 1 = [\ 64.328 + 29498.1/(146 - \lambda^{-2}) + 255.4/(41 - \lambda^{-2})\ ] \times 10^{-6} \qquad (\lambda \text{ in } \mu\text{m})$$

Somewhat inconsistent values of δ have been reported as in Table 1. The Penndorf's value seems to be too large compared with the recent two values.

Table 1. Values of depolarizing factor

Reference		Δ	δ	ratio
Penndorf	1957	0.035	1.0608	1
Hoyt	1977	0.0139	1.0235	0.965
Fröhlich & Shaw	1980	0.0095	1.0160	0.958

References

Allen, C.W.: Astrophysical Quantities, Athlone Press, pp 310 (1976)

Born, M. and E. Wolf: Principles of optics, Pergamon Press, pp 808 (1970)

Fröhlich, C. and G.E. Shaw: New determination of Rayleigh scattering in the terrestrial atmosphere, Appl. Opt., 19, 1773-1775 (1980)

Fynat, A.L. and C.B. Smith: Remote sensing of the middle atmospheric aerosol, Pageoph, 118, 35-57 (1980)

Hoyt, D.V.: A redetermination of the Rayleigh optical depth and its application to selected solar radiation problems, J. Appl. Met., 16, 432-436 (1977)

Kondo, Y. and M. Takagi: Measurement of lower stratospheric aerosol by a balloon-borne photometer, Pageoph, 118, 858-866 (1980)

Kondo, Y., M. Takagi and H. Ishikawa: Balloon observations of stratospheric aerosol and ozone, Bull. Inst. Space Aeron. Sci., Univ. Tokyo, 14, 1195-1202 (1978) (in Japanese)

Kondo, Y., M. Takagi and A. Iwata: Measurements of stratospheric aerosol by balloon-borne sun-photometers, Bull. Inst. Space Astron. Sci., 4, 75-86 (1982a) (in Japanese)

Kondo, Y., M. Takagi and A. Iwata: Measurements of stratospheric ozone by Chappuis band attenuation, Bull. Inst. Space Astron. Sci., 4, 87-91 (1982b) (in Japanese)

Kondo, Y., M. Takagi and A. Iwata: Measurements of stratospheric ozone by Chappuis band absorption, submitted to J. Met. Soc. Japan (1983)

Miller, D.E.: Stratospheric attenuation in the near ultraviolet, Proc. Roy. Soc., A, 301, 57-75 (1967)

Penndorf, R.: Tables of the refractive index for standard air and the Rayleigh scattering coefficient for the spectral region between 0.2 and 20.0 μm and their application to atmospheric optics, J. Opt. Soc. Am., 47, 176-182 (1957)

Pepin, T.J.: Inversion of solar extinction data from the Appolo-Soyuz test project stratospheric aerosol measurement (ASTP/SAM) experiment, in Inversion Methods in Atmospheric Remote Sensing, Academic Press, 529-554 (1977)

Snider, D.E. and A. Goldman: Refractive effects in remote sensing of the atmosphere with infrared transmission spectroscopy, USA Ballistic Research Laboratories Report, No. 1790, pp 153 (1975)

Wang, P.H., A. Deepak and S-S. Hong: General formulation of optical depths for large zenith angles in the earth's curved atmosphere, J. Atm. Sci., 38, 650-658 (1981)